Dalton Transactions

Accepted Manuscript

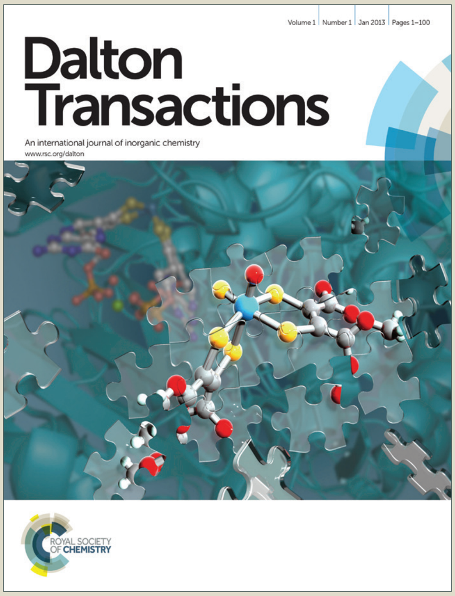

Synthesis, structures and DFT calculations of 2-(4,6-dimethyl pyrimidyl)selenolate complexes of Cu(I), Ag(I) and Au(I) and their conversion into metal selenide nanocrystals

Rakesh K. Sharma,[a] Amey Wadawale,[a] G. Kedarnath,[a] Debashree Manna,[b] Tapan K. Ghanty,[b] B. Vishwanadh[c] and Vimal K. Jain[a]*

[a]*Chemistry Division,* [b]*Theoretical Chemistry Section,* [c]*Materials Science Division, Bhabha Atomic Research Centre, Mumbai- 400 085 (India),*

Tel: +91 22 2559 5095; Fax: +91 22 2550 5151; Email: jainvk@barc.gov.in

The complexes, $[M\{SeC_4H(Me\text{-}4,6)_2N_2\}]_6$ (M = Cu (**1**), Ag (**2**)) and $[Au\{SeC_4H(Me\text{-}4,6)_2N_2\}(PEt_3)]$ (**3**) have been prepared and characterized by elemental analyses, uv-vis, NMR (^1H, ^{13}C, ^{77}Se) spectroscopy and single crystal X-ray diffraction. The crystal structures of $[Cu\{SeC_4H(Me\text{-}4,6)_2N_2\}]_6.H_2O$ (**1**.H_2O), $[Ag\{SeC_4H(Me\text{-}4,6)_2N_2\}]_6$**.**6MeOH.$H_2O$ (**2**.6MeOH.H_2O) and $[Au\{SeC_4H(Me\text{-}4,6)_2N_2\}(PEt_3)]$ (**3**) revealed that their metal centers acquire distorted tetrahedral, trigonal and linear geometries, respectively. DFT calculations have been carried out to rationalize nuclearity in copper(I) chalcogenolate complexes. The calculations suggest that there is hardly any energy difference between the tetrameric and hexameric forms. Thermal behavior of $[Cu\{SeC_4H(Me\text{-}4,6)_2N_2\}]_6$ was studied by thermogravimetric analysis. Thermolysis of $[M\{SeC_4H(Me\text{-}4,6)_2N_2\}]_6$ (M = Cu, Ag) in 1-dodecanethiol (DDT) at 150 °C gave cubic phase of Cu_7Se_4 and orthorhombic phase of Ag_2Se, respectively. Copper selenide (Cu_7Se_4) thin films were deposited on glass and silicon substrates by using $[Cu\{SeC_4H(Me\text{-}4,6)_2N_2\}]_6$ at 400 °C by AACVD.

Introduction

Group-11 metal chalcogenides constitute an interesting family of semiconductor materials exhibiting a wide structural and compositional diversity. Both stoichiometric (e.g., CuE, Cu_2E, Ag_2Se) and non-stoichiometric (e.g., $Cu_{2-x}E$) compositions of metal chalcogenides have been isolated in several crystallographic forms.[1,2] Their unique properties have been exploited for numerous applications in electronic[3], opto-electronic[4] and thermo-electric devices[5,6]. For instance copper chalcogenides find applications in solar cells (e.g., $Cu_{2-x}Se$),[4] thermo electric convertors (Cu_2Te),[7] *etc*. Silver selenide is a useful material for photo-chargeable batteries[8] and thermochromic material in photographic films[9]. Despite their technological utility, synthesis of high quality Group-11 metal chalcogenides remains elusive. Although several methods to prepare copper chalcogenides[10-15] and silver selenide[16-18] have been reported, in general single source molecular precursors route has emerged as a versatile strategy to prepare phase pure chalcogenides with precise control on composition under mild reaction conditions[19,20]. Metal chacogenolates have been successfully used as single source molecular precursors for the synthesis of metal chalcogenide nano-materials. Recently a few examples of copper (e.g. $[Cu\{SeP(OPr^i)_2\}]_4$,[21] $[Cu\{EC_5H_3(R\text{-}3)N\}]_4$ (E = Se or Te),[22] $[Cu_{20}Se_{13}(PEt_3)_{12}]$[23] and silver chalogenolates complexes[24,25] as single source precursors for the preparation of metal chalcogenides have been reported.

Group-11 metals (Cu, Ag, Au) chalcogenolate complexes have been of considerable interest for the past several decades with predominance by thiolate derivatives[26]. There have been several reasons for such an insatiable interest in these complexes. They exhibit an interesting array of geometric configurations varying from mono-nuclear to large clusters,[26] metallophilic M…M (M = Cu, Ag or Au) intermolecular interactions,[27-30] in catalysis for C-S bond cleavage (e.g. desulfurization[31]) and bond formation,[32] in bioinorganic chemistry due to their role in numerous metallo- proteins/ enzymes,[33] gold thiolates in the treatment of arthritis[34, 35] and in materials science[19,20]. Gold alkylselenolates have shown promising potential as heat developable materials in photography[36] and also emerging as GPx inhibitors in biological systems[37].

Copper(I) and silver(I) chalcogenolates exhibit interesting stereochemistry with a wide structural diversity. The nuclearity of these complexes varies between discrete monomeric (e.g., $[Cu(SpymCF_3\text{-}4)(PPh_3)_3]$[38] to octanuclear (e.g. $[Cu_8(\mu\text{-}S)\{S_2P(OPr^i)_2\}_6]$[39] and is influenced by subtle changes in electronic and steric demands of the ligands. For instance, the nature of R group in $[Cu\{S_2P(OR)_2\}]_n$ decides the nuclearity of the complex (R = Et,[39] n = 6; R = Pr^i,[40] n = 4). Similarly the chalcogen atoms in $[Cu(EC_5H_4N)]_n$ (E = S,[41] n = 6; Se,[42] n = 4; Te,[22] n = 4).

Recently a variety of bulky organochalcogen ligands have been employed for the synthesis of metal complexes.[43-45] We have employed 2-(4,6-dimethyl pyrimidyl)selenolate(**I**) for the synthesis of Cu(I), Ag(I) and Au(I) complexes. They have been characterized structurally while copper and silver complexes have been used as precursors for the synthesis of single phased metal chalcogenides. Results of this work are reported herein.

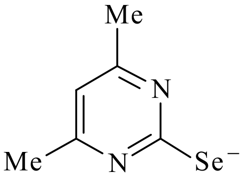

I

Experimental

Materials and Methods

CuCl, $AgNO_3$, $AuCl(PEt_3)$, dodecanethiol (DDT) and analytical grade solvents were obtained from commercial sources. The ligand bis(4,6-dimethyl-2-pyrimidyl)diselenide $[\{Se\text{-}C_4H(Me\text{-}4,6)_2\}_2$; ^1H NMR ($CDCl_3$) δ: 2.37 (s, Me); 6.71 (s, CH-5). $^{13}C\{^1H\}$ NMR ($CDCl_3$) δ: 23.7 (Me); 117.2 (CH-5); 165.7 (C-2); 167.5 (C-4,6). $^{77}Se\{^1H\}$ NMR ($CDCl_3$) δ: 486 ppm] was prepared according to literature method.[46]

Elemental analyses were carried out on a Thermofischer Flash EA1112 elemental analyzer. The ^1H, $^{13}C\{^1H\}$ and $^{77}Se\{^1H\}$ NMR spectra were recorded on a Bruker Avance-II spectrometer operating at 300, 75.47 and 57.24 MHz, respectively. Chemical shifts are relative to internal chloroform peak for ^1H and $^{13}C\{^1H\}$ NMR spectra and external Ph_2Se_2 (δ 463 ppm relative to Me_2Se) in $CDCl_3$ for $^{77}Se\{^1H\}$ NMR spectra. $^{31}P\{^1H\}$ NMR spectra were externally referenced to 85% H_3PO_4. UV-vis absorption spectra were recorded on a JASCO V-630 double beam UV-vis spectrophotometer.

Thermogravimetric analyses (TGA) were carried out on a Nitzsch STA 409 PC-Luxx TG-DTA instrument, which was calibrated with $CaC_2O_4.H_2O$. The TG curves were recorded at a heating rate of 10 ^oC min^{-1} under a flow of argon. X-ray powder diffraction patterns were obtained on a Philips PW-1820 powder diffractometer using CuK_α radiation. SEM and EDX measurements were carried out on MIRERO Inc. AIS2100 and Oxford INCA E350 instruments, respectively. JEOL-2000FX and Tecnai G2 T20 transmission electron microscopes operating at accelerating voltages up to 200 kV were used for TEM studies. The samples for TEM and SAED were prepared by placing a drop of sample dispersed in acetone on a carbon coated copper grid.

X-ray crystallography

Intensity data of $[Cu\{SeC_4H(Me\text{-}4,6)_2N_2\}]_6.H_2O$ (**1**.H_2O), $[Ag\{SeC_4H(Me\text{-}4,6)_2N_2\}]_6.6MeOH.H_2O$ (**2**.6MeOH.H_2O) and $[Au\{SeC_4H(Me\text{-}4,6)_2N_2\}(PEt_3)]$ (**3**) were collected at room temperature (298 K) on a Rigaku AFC7S diffractometer using graphite monochromated Mo K_α ($\lambda = 0.71069$ Å) radiation so that $\theta_{max} = 27.5^\circ$. The unit cell parameters (Table 1) were determined from 25 reflections measured by a random search routine. The intensity data were corrected for Lorentz, polarization and absorption effects with an empirical procedure.[47] The structures were solved by direct methods using SHELX-97[48] and refined by full-matrix least squares methods. The non-hydrogen atoms were refined anisotropically. The hydrogen atoms were fixed in their calculated positions. Molecular structures were drawn using ORTEP.[49]

DFT calculations

Geometry optimizations for all the copper complexes with $EC_4H(Me\text{-}4,6)_2N_2$ (E = S, Se) ligands have been carried out using TURBOMOLE program package.[50] All the atoms were treated at the all electron level and the standard def-TZVP basis sets as implemented in the TURBOMOLE program has been used. Geometries of the bare ligands and their complexes with Cu^+ ion were optimized at the DFT/GGA level of theory using Becke's exchange functional[51] in conjunction with Perdew's correlation functional (BP86)[52]. Geometrical parameters and complexation energy values were calculated for all the complexes. Charge distribution on the metal and donor centers has also been calculated using the natural population analysis scheme for the bare ligand as well as for all the metal complexes.

Syntheses of complexes

[Cu{SeC$_4$H(Me-4,6)$_2$N$_2$}]$_6$ (1). To a freshly prepared NaSeC$_4$H(Me-4,6)$_2$N$_2$ [from toluene-methanol solution of {SeC$_4$H(Me-4,6)$_2$N$_2$}$_2$ (150 mg, 0.40 mmol) and NaBH$_4$ (34 mg, 0.90 mmol) in methanol] was added solid CuCl (79 mg, 0.80 mmol). The whole was stirred at room temperature for 4 h and the solvents were evaporated under vacuum. The residue was washed thoroughly with diethyl ether to remove excess ligand and extracted with dichloromethane and filtered. The filtrate was concentrated under reduced pressure and recrystallized from dichloromethane-methanol mixture to yield yellow crystals (Yield: 158 mg, 79 %), m.p. 138 ^{o}C. Anal. Calcd. for $C_{36}H_{42}Cu_6N_{12}Se_6$: C, 28.87; H, 2.83%. Found: C, 29.05; H, 2.93%. uv-vis λ_{max} (CH_2Cl_2)/nm 257 and 303. ^{1}H NMR ($CDCl_3$) δ: 2.40 (s, 3 H, 4-Me); 2.58 (s, 3 H, 6-Me); 6.77 (s, 1 H, CH-5). ^{13}C{^{1}H} NMR ($CDCl_3$) δ: 24.0 (4-Me); 24.2 (6-Me); 116.2 (CH-5); 165.7; 166.9; 171.4. ^{77}Se{^{1}H} NMR ($CDCl_3$) δ: 122 ppm.

[Ag{SeC$_4$H(Me-4,6)$_2$N$_2$}]$_6$ (2). Prepared similar to **1** employing AgNO$_3$ (429 mg, 2.52 mmol) in toluene-methanol and isolated as yellow crystals (Yield: 549 mg, 74 %), m.p. 180 ^{o}C (dec.). Anal. Calcd. for $C_{36}H_{42}Ag_6N_{12}Se_6$.toluene: C, 27.83; H, 2.71%. Found: C, 27.01; H, 2.72%. uv-vis λ_{max} (CH_2Cl_2)/nm 290. ^{1}H NMR ($CDCl_3$) δ: 2.36 (s, 3 H, 4-Me); 2.39 (s, 3 H, 6-Me); 6.46 (s, 1 H, CH-5); 6.73 (s, 1 H, CH-5). ^{77}Se{^{1}H} NMR ($CDCl_3$) δ: 90 ppm.

[Au{SeC$_4$H(Me-4,6)$_2$N$_2$}(PEt$_3$)] (3). Prepared in a similar fashion to **1** employing AuCl(PEt$_3$) (135 mg, 0.38 mmol) and isolated as yellow crystals (Yield: 100 mg, 70 %), m.p. 208 ^{o}C. Anal. Calcd. for $C_{12}H_{22}AuN_2PSe$: C, 28.76; H, 4.42%. Found: C, 28.14; H, 4.60%. uv-vis λ_{max} (CH_2Cl_2)/nm 286. ^{1}H NMR ($CDCl_3$) δ: 1.25 (m, *CH$_3$*CH$_2$P); 1.86 (m, 6 H, *CH$_2$*P); 2.28 (s, 6 H, Me); 6.62 (s, 1H, CH-5) (ring protons). ^{31}P{^{1}H} NMR($CDCl_3$) δ: 38.2. ^{13}C{^{1}H} NMR ($CDCl_3$) δ: 9.0 (*C*H$_3$CH$_2$P), 18.2 (d, J(P-C) = 32 Hz, *C*H$_2$P), 23.9 (Me), 115.6 (CH-5), 165.8 (C-2), 173.9 (C-4, C-6). ^{77}Se{^{1}H} NMR (CDCl$_3$) δ: 268 ppm.

Preparation of metal selenide nanoparticles

To a pre-heated (170 °C) DDT (3 ml) (**experiment 1**) in a three necked flask, a solution of [Cu{SeC$_4$H(Me-4,6)$_2$N$_2$}]$_6$ (**1**) (70 mg, 0.047 mmol) in a CH$_2$Cl$_2$ (2 cm^3) was injected rapidly with vigorous stirring under flowing argon. The temperature was maintained at 150 °C for 25 min. The hot solution was cooled down rapidly to 70 °C and methanol (20 cm^3) was added so as to get black residue which was washed thoroughly with methanol, followed by centrifuging and drying under vacuum.

In a similar fashion, a suspension of [Ag{SeC$_4$H(Me-4,6)$_2$N$_2$}]$_6$ (**2**) (70 mg, 0.040 mmol) in DDT (2 ml) was injected in DDT (3 ml) and temperature was maintained at 150 °C for 30 minutes and precipitated with methanol, followed by centrifuging and drying under vacuum.

Preparation of Cu$_7$Se$_4$ thin films by AACVD

In a typical experiment precursor **1** (~75 mg) was dissolved in 25 cm^3 of toluene. Aerosol droplets of the solution were generated by an ultrasonic humidifier and were transported using argon as a carrier gas (flow rate of 360 sccm) to a hot glass substrate placed in a turbo furnace.

Results and discussion

Synthesis and Spectroscopy

Treatment of CuCl, AgNO$_3$ and AuCl(PEt$_3$) with one equivalent of sodium 2-(4, 6-dimethyl pyrimidyl)selenolate, NaSeC$_4$H(Me-4,6)$_2$N$_2$, in toluene-methanol gave the corresponding selenolate complexes, [M{SeC$_4$H(Me-4,6)$_2$N$_2$}]$_6$ (M = Cu (**1**), Ag (**2**)) and [Au{SeC$_4$H(Me-4,6)$_2$N$_2$}(PEt$_3$)] (**3**)) (Scheme 1). The electronic spectra displayed a band in the region 286-303 nm which can be assigned to ligand-to-ligand charge transfer transition. The ^{1}H and ^{13}C{^{1}H} NMR spectra of **1** exhibited two separate resonances for methyl groups due to non-equivalence of methyl groups of abridging selenolate ligand while for gold complex (**3**) only one such resonance was observed. The ^{77}Se NMR spectra displayed single resonances which were considerably shielded with respect to the corresponding signal for diselenide. ^{77}Se NMR resonances for complexes containing tridentate bridging selenolate (as in **1** and **2**) appeared at higher field than the signal for monodentate selenolate (as in **3**).

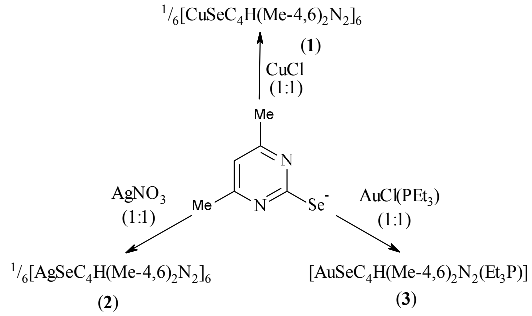

Scheme 1

X-ray Crystallography

The molecular structures of $[Cu\{SeC_4H(Me\text{-}4,6)_2N_2\}]_6.H_2O$ (**1**.H_2O), $[Ag\{SeC_4H(Me\text{-}4,6)_2N_2\}]_6.6MeOH.H_2O$ (**2**.6MeOH.H_2O) and $[Au\{SeC_4H(Me\text{-}4,6)_2N_2\}(PEt_3)]$ (**3**) with atomic numbering scheme are shown in Figs. 1-3. Selected inter-atomic parameters are given in Tables 2 and 3. The complexes **1** and **2** have a hexanuclear structure while complex **3** is a discrete monomer. The former two crystallize with a water molecule and six methanol and a water molecule, respectively.

The copper complex (**1**.H_2O) comprises of an octahedral core of copper atoms which are held together through Cu-Cu bonds and bridging chalcogenolate ligands.

Each copper atom acquires a distorted square-pyramidal configuration defined by the pyrimidyl nitrogen atom, two bridging selenium atoms and two adjacent copper atoms. The Cu-Cu distances vary between 2.7409(17) and 2.8164(17) Å. These distances are longer than those reported in tetranuclear $[Cu\{SeC_5H_3(Me\text{-}3)N\}]_4$ (Cu-Cu = 2.66 Å))[22] and $[Cu\{SeC_5H_3(R\text{-}3)N\}]_4$ (R = H (Cu-Cu = 2.683 Å), $SiMe_3$ (Cu-Cu = 2.73 Å))[42] pyridine-2-selenolate complexes. However these distances are shorter than those reported in hexanuclear pyridine-2-thiolates $[Cu\{SC_5H_3(R\text{-}3)N\}]_6$ (R = H (Cu-Cu(av) = 2.950 Å), $SiMe_3$ (Cu-Cu = 3.139 Å))[53]. Although the Cu-Se (av 2.37 Å) and Cu-N (av 2.02 Å) are well within the range reported for complexes containing Cu-Se and Cu-N bonds, the former is marginally shorter while the latter is slightly longer than those reported in $[Cu\{SeC_5H_3(Me\text{-}3)N\}]_4$ (Cu-Se (av) = 2.40 Å and Cu-N (av) = 2.00 Å))[22] and $[Cu\{Se_2P(OPr^i)_2\}]_4$ (2.354(6)-2.408(5) Å).[21]

The crystal packing diagram along the *b*-axis shows that the molecules are held together in a 3D structure through hydrogen bonding between water molecules and pyrimidyl nitrogen O1…N2 = 3.022 Å and O1…N6 = 3.964 Å (Fig. 1b). The pyrimidal nitrogen of one molecule makes a short contact with hydrogen (H15) atom of pyrimidine ring (C3) of adjacent molecule (N4-H3 = 2.459 Å) on one side and pyrimidyl nitrogen N4 with methyl group C6 on another side (N6…H6c = 2.555 Å).

The molecular structure of silver complex (**2.**$6MeOH.H_2O$) consists of two hexagonal Ag_3Se_3 rings which are inter-connected through bridging selenolate ligands and are arranged in a staggered conformation. In each ring silver and selenium atoms are alternatively arranged. Each silver atom adopts a distoreted trigonal geometry defined by two bridging selenium atoms and the nitrogen atom from third selenolate ligand. The two Ag-Se bonds are distinctly different (2.5337(10), 2.6158(11) Å) and lie within the range reported in $[Ag\{SeC_5H_3(SiMe_3\text{-}6)N\}]_6$ (2.5943(14) - 2.6044(13)

Å)[54]. The Ag-N bond distances (2.329(5) Å) can be compared with those observed in [Ag{$SeC_5H_3(SiMe_3$-6)N}]$_6$ (2.320(6) - 2.386(6) Å)[54] and [Ag(SC_5H_4N)]$_6$ (2.367(5) Å)[28].

The pryrimidyl rings of the two Ag_3Se_3 fragments are almost mutually parallel with the inter-planar distance of 3.501 Å between the two adjacent rings. The silver atoms of each ring make two distinct Ag…Ag contacts (2.8141(12) and 3.2573(13) Å) of the opposite ring, which are shorter than the sum of van der Waals radii of two silver atoms (3.4 Å) indicative of weak metal…metal interaction. These contacts can be compared with those found in other silver chalcogenolates, *e.g.* [Ag{$SeC_6H_2(Pr^i$-2,4,6)$_3$}$_8$] (Ag…Ag = 2.885(2) - 3.258(1) Å)[55] and [Ag(SC_5H_4N)]$_6$ (2.959(2) - 3.369(3) Å)[28].

The molecules are held together in three dimensional structures through hydrogen bonds between hydroxyl proton of methanol molecules with pyrimidal nitrogen (N2---H1s = 2.199 Å) on one side and methyl group of pyrimidine rings (O1s---H6A = 2.621 Å) on another side (Fig. 2b). These molecules are arranged in vertical concentric columns along c–axis in a staggered conformation. A water molecule is sandwiched between two hexanulcear silver complex along with six methanol molecules (3 each from adjacent AgSe molecules) arranged in a hexagonal fashion around it. The water molecule is concentric with the center of the AgSe molecules (Fig. 2c) and lies exactly in the center of hexagon formed by methanol molecules. It is coplanar with the methyl carbon of the six methanol molecules (Fig 2d).

Gold in complex **3** is two coordinated and adopts nearly a linear (P1 –Au1–Se1 = 175.37(18)°) geometry as is observed for Au(I) chalcogenolate complexes[56,57]. The Au-Se and Au-P bond distances are as expected and are similar to those reported in [Au(SePh)(PPh_3)] (Au-Se = 2.415(2) Å),[58] [Au($SeC_2B_{10}H_{11}$)(PPh_3)] (Au-Se = 2.4167(4) Å, Au-P = 2.2690(10) Å),[59] and [Au_2{$SeC_6H_4(CH_2NMe_2)$-2}$_2$(μ-dppe)] (Au-Se = 2.404(1) Å, Au-P = (2.262(2) Å)[29]. The crystal packing diagram shows the existence of short range inter-molecular interactions. There is a short Au…Au (3.251(2) Å) contacts as can be noted in [Au($SeC_2B_{10}H_{11}$)(PPh_3)] (3.3035(4) Å)[59]. The observed Au…Au contacts are, however, longer than those reported in [Au(SePh)(PPh_3)] (Au…Au) = 3.118(1) Å)[58] and [{Au(SePh)}$_2$(dppe)] (Au---Au = 3.044(9) Å)[60]. Gold atom of one molecule forms a secondary bond with selenium atom of adjacent molecule (Au…Se = 3.475 Å) resulting in a four-membered rectangular Au_2Se_2 core. Besides these secondary interactions, the C-1 atom of seleno pyrimidyl ring of this formal dimeric unit makes weak contact with the methyl hydrogen (H3) of the adjacent dimeric unit generating a 1-D supra-molecular assembly.

DFT calculations

Copper pyridyl thiolates, irrespective of the substituents in the pyridyl ring exist in hexameric form, whereas the heavier pyridyl chalogenolates (Se[22, 42] or Te[22]) adopt a tetrameric structure. Analogously, the pyrimidyl thiolate acquires a hexameric form.[38] In contrast, the pyrimidyl selonate, discussed here adopts a hexameric structure. This led us to examine the factors responsible in defining nuclearity of the complex. Additionally, nitrogen atom in the pyrimidyl ring reduces the electron density on the chalcogen atoms.

The optimized structures of the bare ligands and complexes have been depicted in Figs. 4 and 5. All the calculated metal-ligand bond distances, the complexation energy values and charges on copper and the donor centers are given in Tables 4 and 5, respectively. Apparently from the calculated metal-ligand bond distances no definitive trend was noted which could rationalize the experimentally observed results. However, from the charge values on the N and S/Se centers corresponding to the bare ligands (Table 6) it can be found that the charge values on the S/Se atom is rather dependent on the number of nitrogen atoms present in the ligand. Also, the charge values on the S and Se atoms are almost the same for both pyridyl and pyrimidyl based ligands. Nevertheless, from the calculated complexation energy values reported in Table 4 it is evident that the difference in the complexation energy between the hexameric selonate complexes involving pyridyl and pyrimidyl ligands is slightly larger as compared to the corresponding hexameric thiolate complexes. The hexameric pyrimidyl selonate complex is associated with higher complexation energy, which is consistent with the experimentally observed results. On the other hand, hexameric pyridyl thiolate and the hexameric pyrimidyl thiolate have almost the same complexation energy values, which can rationalize the observation of hexameric complexes involving both the pyridyl and the pyrimidyl ligands in the case of thiolate complexes. However the experimental observation of tetrameric complex in case of 3-methyl-2-pyridyl selenolate cannot be explained through theoretically obtained results. Here all the calculations have been carried out at the molecular level using finite systems instead of using periodic approach. Therefore, apart from the reported theoretical parameters, either crystal packing effects, which are hard to evaluate, or the presence of more than one electronegative atom (nitrogen) in the aryl ring may be responsible for the experimentally observed results. Additionally, hydrogen bonding in the crystal may also play an important role in stabilizing a hexameric structure. Nevertheless, molecular structures and complexation energy values obtained using DFT calculations using first principle approach are also useful in understanding the metal-ligand specific interactions at the molecular level.[61]

Thermal studies

The TG curve (Fig. 6) of $[Cu\{SeC_4H(Me\text{-}4,6)_2N_2\}]_6$ (**1**) shows a single step decomposition with the formation of a black residue. The latter could be Cu_7Se_4 as inferred from weight loss (found 57.6%, calcd. for the formation of Cu_7Se_4 56.5%).

Copper and silver nanostructures

Thermolysis of **1** and **2** in dodecylthiol (DDT) at 150 ^{o}C gave black flocculates which were characterized by XRD, EDX, SEM and TEM techniques. The XRD patterns (Figs. 7 and 8) showed peaks which could be indexed to the cubic phase of Cu_7Se_4 (JCPDS file No. 26-0557) and orthorhombic phase of Ag_2Se (JCPDS file No. 24-1041). The EDX analyses (Cu:Se atom ratio = 20.9 : 11.5 (Cu/Se =1.8); Ag:Se atom ratio = 67.3 : 32.7 (Ag/Se = 2.06)) are consistent with Cu_7Se_4 and Ag_2Se compositions.

The SEM images of both the selenides show spherical shaped aggregated structures. TEM micrograph of Cu_7Se_4 showed the presence of irregular shaped nano-crystals of 100-500 nm diameter. Discrete spots in SAED pattern (Fig 7d) confirmed their single phased crystalline nature. The TEM image of Ag_2Se revealed the existence of a mixture of spherical and ellipsoid shaped nano-crystals with the sizes 110-170 nm and 100 x 200 nm, respectively.

Copper selenide thin films

Copper selenide thin films were deposited on glass and silicon substrates using $[Cu\{SeC_4H(Me\text{-}4,6)_2N_2\}]_6$ (**1**) at 400 ^{o}C for 3h. XRD patterns (supporting information) and EDX analyses [Cu:Se atom ratio is 64.5 : 35.5 (Cu/Se = 1.81)] of the films showed that they corresponds to cubic phase of Cu_7Se_4 (JCPDS File No. 26-

0557, cell parameter a = 11.41) (Fig. 9). The XRD patterns showed well defined peaks suggesting that the films are crystalline. The films deposited on glass substrate grew preferentially in (222) direction while films deposited on silicon substrate grew preferentially in (440) direction. SEM image (Fig. 9b) of the Cu_7Se_4 film grown on glass substrate showed wool like structures while films deposited on silicon substrate comprised of high quality vertically oriented hexagonal sheets. The effect of substrate on morphology of metal selenide thin films has been noted earlier.[62]

Conclusion

4,6-Dimethylpyrimidyl selenolates of Cu(I), Ag(I) and Au(I) have been conveniently synthesized and isolated as air stable complexes. DFT calculations in copper chalcgenolate complexes revealed that there is hardly any energy difference between tetramric and hexameric forms. The copper and silver complexes are versatile single source molecular precursors which can be used for facile synthesis of Cu_7Se_4 and Ag_2Se nanomaterials. The copper complex has also been employed for deposition of Cu_7Se_4 thin films by AACVD.

Acknowledgements

One of the authors (RKS) is thankful to CSIR, New Delhi for the award of a Senior Research Fellowship to him.

Supporting Information

CCDC-Nos. 963090, 963091 and 963092 for $[Cu\{SeC_4H(Me\text{-}4,6)_2N_2\}]_6.H_2O$ (**1**.H_2O), $[Ag\{SeC_4H(Me\text{-}4,6)_2N_2\}]_6.6MeOH.H_2O$ (**2**.6MeOH.H_2O) and $[Au\{SeC_4H(Me\text{-}4,6)_2N_2\}(PEt_3)]$ (**3**) respectively contains the supplementary crystallographic data for this paper. These data can be obtained free of charge at www.ccdc.cam.ac.uk/conts/retrieving.html or from the Cambridge Crystallographic Data Centre, 12 Union Road, Cambridge CB2 1EZ, UK [Fax: + 44-1223/336-033; E-mail: deposit@ccdc.cam.ac.uk].

References

1 A. L .N. Stevels and F. Jellinek, *Recueil*, 1971, **111**, 273.

2 A. L. N. Stevels and G. A. Wiegers, *Recl. Trav. Chim. Puys-Bas*, 2010, **90**, 352.

3 H. Toyoji and Y. Hiroshi, *Jpn, Kokai Tokkyo Koho*, 1990, JP02173622.

4 S. Y. Zhang, C. X. Fang, Y. P. Tian, K. R. Zhu, B. K. Jin, Y. -H. Shen and J. X. Yang, *Cryst. Growth Des.*, 2006, **6**, 2809.

5 J. J. Ritter and P. Maruthamuthu, *Inorg. Chem.*, 1995, **34**, 4278.

6 T. Chivers, *J. Chem. Soc., Dalton Trans.*, 1996, 1185.

7 K. Sridhar and K. Chattopadhyay, *J. Alloys Compd.*, 1998, **264**, 293.

8 B. Gates, Y. Wu, Y. Yin, P. Yang and Y. Xia, *J. Am. Chem. Soc.*, 2001, **123**, 11500.

9 B. Gates, B. Mayers, Y. Wu, Y. Sun, B. Cattle, P. Yang and Y. Xia, *Adv. Funct. Mater.*, 2002, **12**, 679.

10 T. Ohtani, M. Motoki, K. Koh and K. Oshima, *Mater. Res. Bull.*, 1995, **30**, 1495.

11 G. Henshaw, I. P. Parkin and G. A. Shaw, *J. Chem. Soc., Dalton Trans.*, 1997, 231.

12 W. Wang, P. Yan, F. Liu, Y. Xie, Y. Geng and Y. Qian, *J. Mater. Chem.*, 1998, **8**, 2321.

13 W. Wang, Y. Geng, P. Yan, F. Liu, Y. Xie, Y. Qian, *J. Am. Chem. Soc.*, 1999, **121**, 4062.

14 Y. Xie, X. Zheng, X. Jiang, J. Lu and L. Zhu, *Inorg. Chem.*, 2002, **41**, 387.

15 P. Kumar and K. Singh, *Cryst. Growth Des.*, 2009, **9**, 3089.

16 G. Sáfrán, O. Geszti, G. Radnóczi, P. B Barna, *Thin Solid films*, 1998, **317**, 72.

17 R. Harpeness, O. Palchik, A. Gedanken, V. Palchik, S. Amiel, M. A. Slifkin, and A. M. Weiss, *Chem. Mater.*, 2002, **14**, 2094.

18 A. Sahu, L. Qi, M. S. Kang, D. Deng and D. J. Norris, *J. Am. Chem. Soc.*, 2011, **133**, 6509.

19 M. Bochmann, *Chem. Vap. Dep.*, 1996, **2**, 85.

20 M. A. Malik, M. Afzaal and P. O'Brien, *Chem. Rev.*, 2010, **110**, 4417-4446.

21 Y. -J. Hsu, C. M. Hung, Y. F. Lin, B. J. Liaw, T. S. Lobana, S. Y. Lu and C. W. Liu, *Chem. Mater.*, 2006, **18**, 3323.

22 R. K. Sharma, G. Kedarnath, V. K. Jain, A. Wadawale, C. G. S. Pillai, M. Nalliath and B. Vishwanadh, *Dalton Trans.*, 2011, **40**, 9194.

23 A. Eichhöfer, D. Fenske and P. Scheer, *Eur. J. Inorg. Chem.*, 2004, 93.

24 M. T. Ng, C. Boothroyd and J. J. Vittal, *Chem. Commun.*, 2005, 3820.

25 H. Joshi, K. N. Sharma, V. V. Singh, P. Singh and A. K. Singh, *Dalton Trans.*, 2013, **42**, 2366.

26 I. G. Dance, *Polyhedron*, 1986, **5**, 1037.

27 G. K. Batsala, V. Dokorou, N. Kourkoumelis, M. J. Manos, A. J. Tasiopoulos, T. Mavromoustakos, M. Simčič, S. G. - Grdadolnik, S. K. Hadjikakou, *Inorg. Chim. Acta*, 2012, **382**, 146.

28 M. Hong, W. Su, R. Cao, W. Zhang and J. Lu, *Inorg. Chem.*, 1999, **38**, 600.

29 O. Crespo, M. C. Gimeno, A. Laguna, M. Kulcsar and C. Silvestru, *Inorg. Chem.*, 2009, **48**, 4134.

30 H. Schmidbaur and A. Scheir, *Chem. Soc. Rev.*, 2008, **37**, 1931.

31 M. D. Curtis and S. H. Druker, *J. Am. Chem. Soc.*, 1997, *119*, 1027.

32 D. S. Glueck, *Dalton Trans.*, 2008, 5276.

33 G. Henkel and B. Krebs, *Chem. Rev.*, 2004, **104**, 801.

34 E. R. T. Tiekink, *Gold Bulletin*, 2003, *36*, 117.

35 C. F. ShawIII, *Chem. Rev.*, 1999, **99**, 2589; R. Bau, *J. Am. Chem. Soc.*, 1998, **120**, 9380.

36 A. Molter and F. Mohr, *Coord. Chem. Rev.*, 2010, **254**, 19.

37 K. P. Bhabak and G. Mugesh, *Inorg. Chem.*, 2009, **48**, 2449.

38 A. Rodriguez, A. Sousa-Pedrares, J. A. Garcia-Vazquez, J. Romero and A. Sousa, *Eur. J. Inorg. Chem.*, 2011, 3403.

39 C. W. Liu, T. Stubbs, R. J. Staples and J. P. Fackler Jr., *J. Am. Chem. Soc.*, 1995, **117**, 9778.

40 S. L. Lawton, W. J. Rohrbaugh and G. T. Kokotailo, *Inorg. Chem.*, 1972, **11**, 612.

41 S. Kitagawa, M. Munakata, H. Shimono, S. Matsuyama and H. Masuda, *J. Chem. Soc., Dalton Trans.*, 1990, 2105.

42 Y. Cheng, T. J. Emge and J. G. Brennan, *Inorg. Chem.*, 1996, **35**, 7339.

43 J. Hu, G. Liu, Q. Jiang, R. Zhang, W. Huang and H. Yan, *Inorg. Chem.*, 2010, **49**, 11199.

44 Y. Zhang, X. Tang, J. Yang, Y. Li, H. Yan and V. I. Bregadze, *Organometallics*, 2013, **32**, 2014.

45 L. Jain, V. K. Jain, N. Kushwah, M. K. Pal, A. P. Wadawale, V. I. Bregadze and S. A. Glazum, *Coord. Chem. Rev.*, 2014, **258-259**, 72.

46 R. S. Chauhan, R. K. Sharma, G. Kedarnath, D. B. Cordes, A. M. Z. Slawin, V. K. Jain, *J. Organomet. Chem.*, 2012, **717**, 180.

47 T. Higashi, *ABSCOR-Empirical Absorption Correction based on Fourier Series Approximation*, Rigaku Corporation, 3-9-12 Matsubara, Akishima, Japan, 1995.

48 G. M. Sheldrick, *SHELX 97-Program for Crystal Structure Analysis*, Göttingen, Germany, 1997.

49 C. K. Johnson, *ORTEP II, Report ORNL-5136*, Oak Ridge National Laboratory, Oak Ridge TN, 1976.

50 R. Ahlrichs, M. Bär, M. Häser, H. Horn, C. Kölmel, *Chem. Phys. Lett.*, 1989, **162**, 165.

51 A. D. Becke, *Phys. Rev. A*, 1988, **38**, 3098.

52 J. P. Perdew, *Phys. Rev. B*, 1986, **33**, 8822.

53 E. Block, M. Gernon, H. Kang and J. Zubieta, *Angew. Chem. Int. Ed. Engl.*, 1988, **27**, 1342.

54 A. Rodriguez, J. Romero, J. A. Garcia-Vázquez, M. L. Durán, A. Sousa-Pedrares, A. Sousa, J. Zubieta, *Inorg. Chim. Acta*, 1999, **284**, 133.

55 K. Tang, X. Jin, H. Yan, X. Xie, C. Liu and Q. Gong, *J. Chem. Soc., Dalton Trans.*, 2001, 1374.

56 P. Pyykkö, *Angew. Chem. Int. Ed.*, 2004, **43**, 4412.

57 M. T. Räisänen, N. Runeberg, M. Klinga, M. Nieger, M. Bolte, P. Pyykkö, M. Leskela and T. Repo, *Inorg. Chem.*, 2007, **46**, 9954.

58 P. G. Jones and C. Thone, *Chem. Ber.*, 1990, **123**, 1975.

59 S. Canales, O. Crespo, M. C. Gimeno, P. G. Jones, A. Laguna and P. Romero, *Dalton Trans.*, 2003, 4525.

60 W. Eikens, C. Kienitz, P. G. Jones and C. Thone, *J. Chem. Soc., Dalton Trans.*, 1994, 83.

61 M. K. Pal, N. Kushwah, D. Manna, A. Wadawale, V. Sudarsan, T. K. Ghanty, and V. K. Jain, *Organometallics*, 2013, **32**, 104.

62 R. K. Sharma, G. Kedarnath, A. Wadawale, C. A. Betty, B. Vishwanadh and V. K. Jain, *Dalton Trans.*, 2012, **41**, 12129.

Table 1. Crystallographic and structural determination data for [Cu{$SeC_4H(Me\text{-}4,6)_2N_2$}]$_6$.$H_2O$ (**1**.H_2O), [Ag{$SeC_4H(Me\text{-}4,6)_2N_2$}]$_6$.6MeOH.$H_2O$ (**2**.6MeOH.H_2O) and [Au{$SeC_4H(Me\text{-}4,6)_2N_2$}($PEt_3$)] (**3**).

Complex	[Cu{$SeC_4H(Me\text{-}4,6)_2N_2$}]$_6$.$H_2O$ (**1**.H_2O)	[Ag{$SeC_4H(Me\text{-}4,6)_2N_2$}]$_6$.6MeOH.$H_2O$ (**2**.6MeOH.H_2O)	[Au{$SeC_4H(Me\text{-}4,6)_2N_2$}($PEt_3$)] (**3**)
Chemical formula	$C_{36}H_{42}Cu_6N_{12}Se_6.H_2O$	$C_{36}H_{42}Ag_6N_{12}Se_6.6MeOH.H_2O$	$C_{12}H_{22}AuN_2PSe$
Formula weight	1515.87	1974.06	501.21
Crystal size/mm^3	0.20× 0.20× 0.20	0.40× 0.40× 0.40	0.15× 0.10× 0.10
Crystal system / space group	Monoclinic/$P2_{1/n}$	Trigonal/R„*c*	Tetragonal/$P4_12_1$ 2
Unit cell dimensions			
a/Å	12.0837(19)	22.157(6)	8.900(5)
b/Å	18.286(5)	22.157(6)	8.900(5)
c/Å	12.1000(13)	22.197(6)	42.382(14)
α	90.00	90.00	90.00
β	107.492(11)	90.00	90.00
γ	90.00	120.00	90.00
Volume/Å^3	2550.0(8)	9437(4)	3357(3)
Z	2	6	8
D_c/g cm^{-3}	1.972	2.082	1.983

μ/mm^{-1}/F(000)	6.780/1456	5.354/ 5664	11.012/1888
Limiting indices	$-15 \leq h \leq 8$; $-23 \leq k \leq 0$; $-15 \leq l \leq 15$	$-24 \leq h \leq 24$; $0 \leq k \leq 28$; $-28 \leq l \leq 16$	$-6 \leq h \leq 11$; $0 \leq k \leq 8$; $-30 \leq l \leq 55$
□ range of data of collection	2.84 to 27.50	2.81 to 27.50	2.70 to 27.48
No. of reflections collected / unique	2230/ 5851	985/2418	1123/2549
No. of data / restraints / parameters	5851/0/250	2418/0/115	2549/1/ 142
Final R_1, ωR_2 indices $[I > 2\sigma(I)]$	0.0537, 0.1148	0.0389, 0.0713	0.0422, 0.0818
R_1, ωR_2 (all data)	0.2159, 0.1592	0.1536, 0.0968	0.1921, 0.1190
Goodness of fit on F^2	0.960	0.928	1.003

Table 2. Selected bond lengths (Å) and angles (^{o}) for $[Cu\{SeC_4H(Me\text{-}4,6)_2N_2\}]_6.H_2O$ (**1**.H_2O).

Cu1-Cu2	2.7406(19)	Cu2^{i}-Cu3	2.8149(19)
Cu1-Cu3	2.7848(18)	Cu3^{i}-Cu2	2.8149(19)
Cu1-Se1	2.3550(17)	Cu3-Se3	2.3616(17)
Cu1-Se2	2.3590(17)	Cu2^{i}-Se2	2.3730(16)
Cu2-Se3	2.3565(17)	Cu3^{i}-Se1	2.3823(16)
Se1^{i}-Cu3	2.3823(16)	Se2^{i}-Cu2	2.3730(16)
Cu1-N1	2.018(5)	Cu2-N3	2.012(5)
Cu3-N5	2.022(6)	Se2-C13	1.810(6)
Se1-C7	1.810(5)	Se3-C1	1.830(4)
Se2-Cu1-Cu2	133.47(7)	Se3^{i}-Cu3-Cu1	71.43(5)
Se1-Cu1-Cu2	74.52(5)	Se1-Cu3-Cu1	136.38(7)
N1-Cu1-Cu2	96.26(19)	N5-Cu3-Cu1	95.8(2)
Se2-Cu1-Cu3	72.89(5)	Se3-Cu3-Cu2^{i}	136.68(7)
Se1-Cu1-Cu3	133.94(7)	Se1^{i}-Cu3-Cu2^{i}	72.70(5)
N1-Cu1-Cu3	93.26(18)	N5-Cu3-Cu2^{i}	87.1(2)
Cu2-Cu1-Cu3	74.37(5)	Cu1-Cu3-Cu2^{i}	76.70(5)
N1-Cu1-Se1	123.18(18)	Se3-Cu3-Se1^{i}	112.84(7)
Se1-Cu1-Se2	106.99(7)	N5-Cu3-Se1^{i}	112.66(19)
N1-Cu1-Se2	117.63(18)	N5-Cu3-Se3	124.2(2)
Se3-Cu2-Cu1	72.33(5)	C7-Se1-Cu1	106.7(2)
Se2^{i}-Cu2-Cu1	131.84(7)	Cu1-Se1-Cu3^{i}	89.39(6)
N3-Cu2-Cu1	96.13(19)	C13-Se2-Cu2^{i}	99.8(2)
Se3-Cu2-Cu3^{i}	132.41(7)	C13-Se2-Cu1	105.1(2)
Se2^{i}-Cu2-Cu3^{i}	72.12(5)	Cu1-Se2-Cu2^{i}	94.48(6)
N3-Cu2-Cu3^{i}	89.28(19)	C7-Se1-Cu3^{i}	99.8(2)
Cu1-Cu2-Cu3^{i}	73.69(5)	C1-Se3-Cu2	105.4(2)
Se3-Cu2-Se2^{i}	108.93(6)	C1-Se3-Cu3	104.8(2)
N3-Cu2-Se2^{i}	116.16(18)	Cu2-Se3-Cu3	90.12(6)
N3-Cu2-Se3	126.47(18)		

Table 3**.** Bond lengths (Å) and angles (^{o}) for $[\mathrm{Ag\{SeC_4H(Me\text{-}4,6)_2N_2\}}]_6.6\mathrm{MeOH.H_2O}$ (**2.**6MeOH.H$_2$O).

Ag1-Ag1^{i}	3.2573(13)	Ag1-Ag1^{iv}	2.8141(12)
Se1-Ag1^{i}	2.6158(11)	Se1-Ag1^{iv}	2.5337(10)
Ag1-Se1^{i}	2.6158(11)	Ag1-Se1^{iv}	2.5337(10)
N1-Ag1	2.329(5)	C1-Se1	1.899(7)
Ag1 ^{iv}-Se1-Ag1^{i}	88.64(3)	N1-Ag1-Ag1^{i}	82.52(13)
Se1 ^{iv}-Ag1-Ag1^{iv}	77.84(3)	N1-Ag1-Se1^{i}	101.28(13)
Se1^{i}-Ag1-Ag1^{iv}	136.02(2)	C2-N1-Ag1	124.3(5)
Se1 ^{iv}-Ag1-Se1^{i}	115.00(4)	C1-Se1-Ag1^{i}	96.71(18)
Se1^{iv}-Ag1-Ag1^{i}	132.53(2)	N1-Ag1-Ag1^{iv}	93.41(13)
Se1^{i}-Ag1-Ag1^{i}	68.97(3)	N1-Ag1-Se1^{iv}	135.93(13)
Ag1^{iv}-Ag1-Ag1^{i}	72.27(3)	C1-N1-Ag1	116.6(4)
		C1-Se1-Ag1^{iv}	112.5(2)

Table 4. Calculated Cu-Cu and Cu-Se /Cu-S bond distances (Å) and complexation energies (eV) for all complexes.

Copper complex	Nuclearity	Cu-Cu	Cu-Se /Cu-S	Total Complexation Energy (in eV)
Pyridyl selenolate	Tetrameric	2.571/2.720	2.436	-43.39
Pyrimidyl selenolate	Tetrameric	2.567/ 2.736	2.435	-43.61
Pyridyl selenolate	Hexameric	2.680	2.416	-64.96
Pyrimidyl selenolate	Hexameric	2.694	2.419	-65.26
Pyridyl thiolate	Tetrameric	2.565/2.738	2.321	-43.44
Pyrimidyl thiolate	Tetrameric	2.565/ 2.737	2.322	-43.52
Pyridyl thiolate	Hexameric	2.672	2.304	-65.35
Pyrimidyl thiolate	Hexameric	2.680	2.301	-65.39

Table 5. Calculated atomic charges on metal and donor centers for all complexes.

Copper complex	Nuclearity	N	Cu	Se/S
Pyridyl selenolate	Tetrameric	-0.568	0.634	-0.326
Pyrimidyl selenolate	Tetrameric	-0.450/-0.600	0.620	-0.299
Pyridyl selenolate	Hexameric	-0.559	0.660	-0.352
Pyrimidyl selenolate	Hexameric	-0.593/-0.455	0.662	-0.338
Pyridyl thiolate	Tetrameric	-0.559	0.677	-0.395
Pyrimidyl thiolate	Tetrameric	-0.441/-0.592	0.666	-0.367
Pyridyl thiolate	Hexameric	-0.552	0.680	-0.400
Pyrimidyl thiolate	Hexameric	-0.586 /-0.447	0.690	-0.390

Table 6. Calculated atomic charges on the donor centers of the bare ligands.

Charge	Pyridyl selenolate	Pyrimidyl selenolate	Pyridyl thiolate	Pyrimidyl thiolate
N	-0.448	-0.472	-0.449	-0.479
Se/S	-0.450	-0.398	-0.434	-0.380

Figure Captions

Fig. 1 (a) Crystal structure of $[Cu\{SeC_4H(Me\text{-}4,6)_2N_2\}]_6.H_2O$ (**1**.H_2O) with atomic number scheme (ellipsoids with 25 % probability) (b) packing along b-axis (c) hydrogen bonding and short contacts.

Fig. 2 (a) Crystal structure of $[Ag\{SeC_4H(Me\text{-}4,6)_2N_2\}]_6.6MeOH.H_2O$ (**2**.6MeOH.H_2O) with atomic number scheme (ellipsoids with 25 % probability) (hydrogen atoms, methanol and water molecules are exclude for clarity) (b) packing along *b*-axis plane (c) packing along *c*-axis (d) arrangement of water molecule with respect to methanol molecules and AgSe molecule.

Fig. 3 (a) Crystal structure of $[Au\{SeC_4H(Me\text{-}4,6)_2N_2\}(Et_3P)]$ (**3**) with atomic number scheme. The ellipsoids were drawn at the 50 % probability. Selected interatomic parameters: Au1– P1 = 2.276(6) Å, Au1– Se1 = 2.418(3) Å, Au1– Au1 = 3.251(2) Å, Se1– C1 = 1.88(2) Å, ∠P1 –Au1– Se1 = 175.37(18), ∠P1– Au1– Au1 = 110.58(17) ^{o}, ∠Se1– Au1– Au1 = 175.37(18) ^{o} and ∠C1– Se1– Au1 = 102.8(8) ^{o}. (b) intermolecular interaction.

Fig. 4 Optimized structures of bare ligands.

Fig. 5 Optimized structures of copper pyridyl/ pyrimidyl selenolates.

Fig. 6 TG curve of $[Cu\{SeC_4H(Me\text{-}4,6)_2N_2\}]_6$ (**1**).

Fig. 7 a) XRD pattern, b) SEM image, c) TEM image and d) SAED pattern of Cu_7Se_4 obtained by the pyrolysis of $[Cu\{SeC_4H(Me\text{-}4,6)_2N_2\}]_6$ (**1**) in DDT at 150 ^{o}C for 25 min.

Fig. 8 a) XRD pattern, b) SEM image and c) TEM image of Ag_2Se obtained by the pyrolysis of $[Ag\{SeC_4H(Me\text{-}4,6)_2N_2\}]_6$ (**2**) in DDT/DDT at 150^{o}C for 30 min.

Fig. 9 **(**a) XRD pattern and b) SEM image of copper selenide (Cu_7Se_4) thin film obtained by AACVD of $[Cu\{SeC_4H(Me\text{-}4,6)_2N_2\}]_6$ (**1**) 400 ^{o}C for 3 h on glass substrate; (c) XRD and (d) SEM image of Cu_7Se_4 thin film obtained by AACVD of $[Cu\{SeC_4H(Me\text{-}4,6)_2N_2\}]_6$ (**1**) 400 ^{o}C for 3 h on silicon substrate.

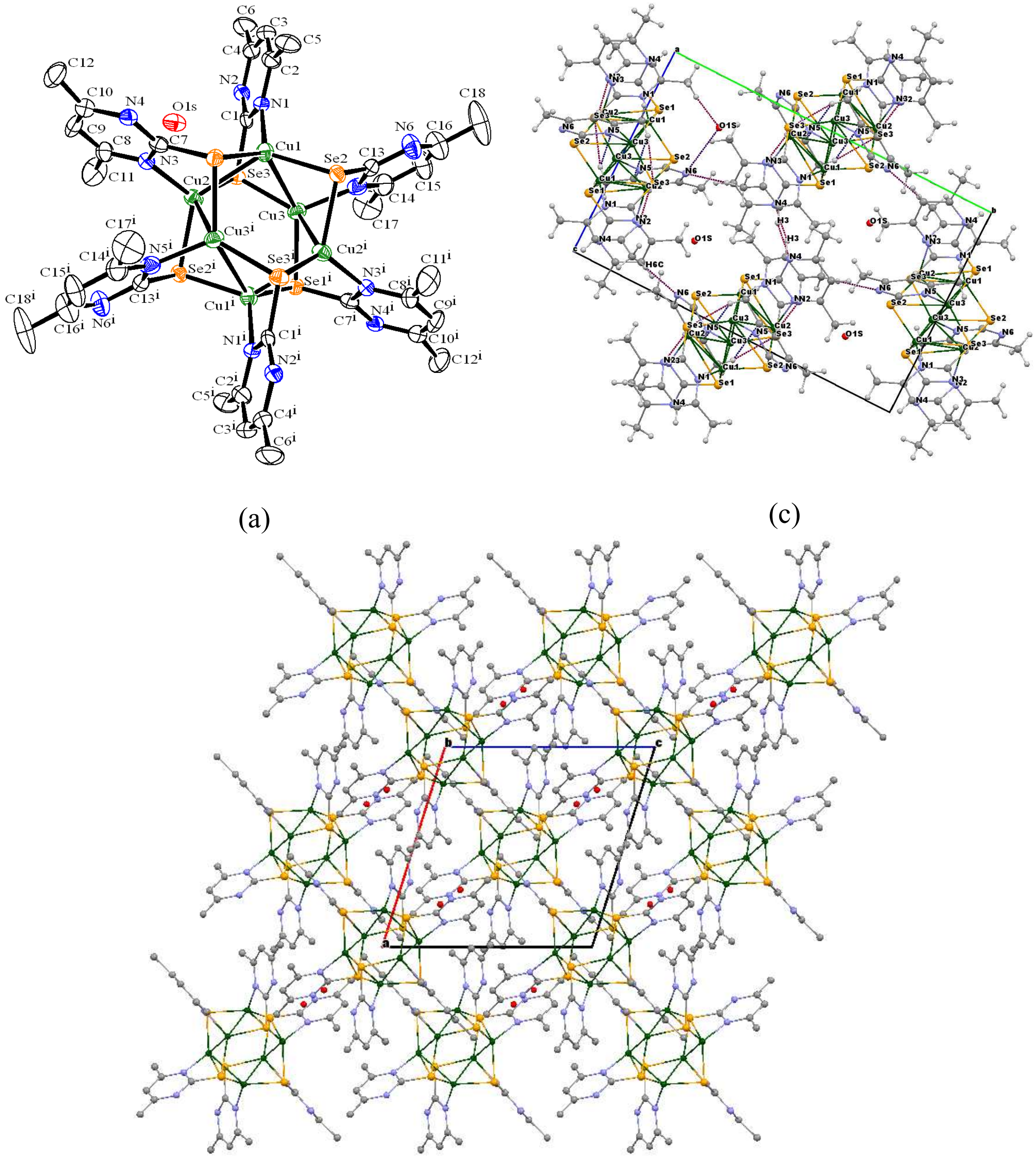

(a)

(c)

(b)

Fig. 1 (a) Crystal structure of $[Cu\{SeC_4H(Me\text{-}4,6)_2N_2\}]_6.H_2O$ (**1**.H_2O) with atomic number scheme (ellipsoids with 25 % probability) (b) packing along b-axis (c) hydrogen bonding and short contacts.

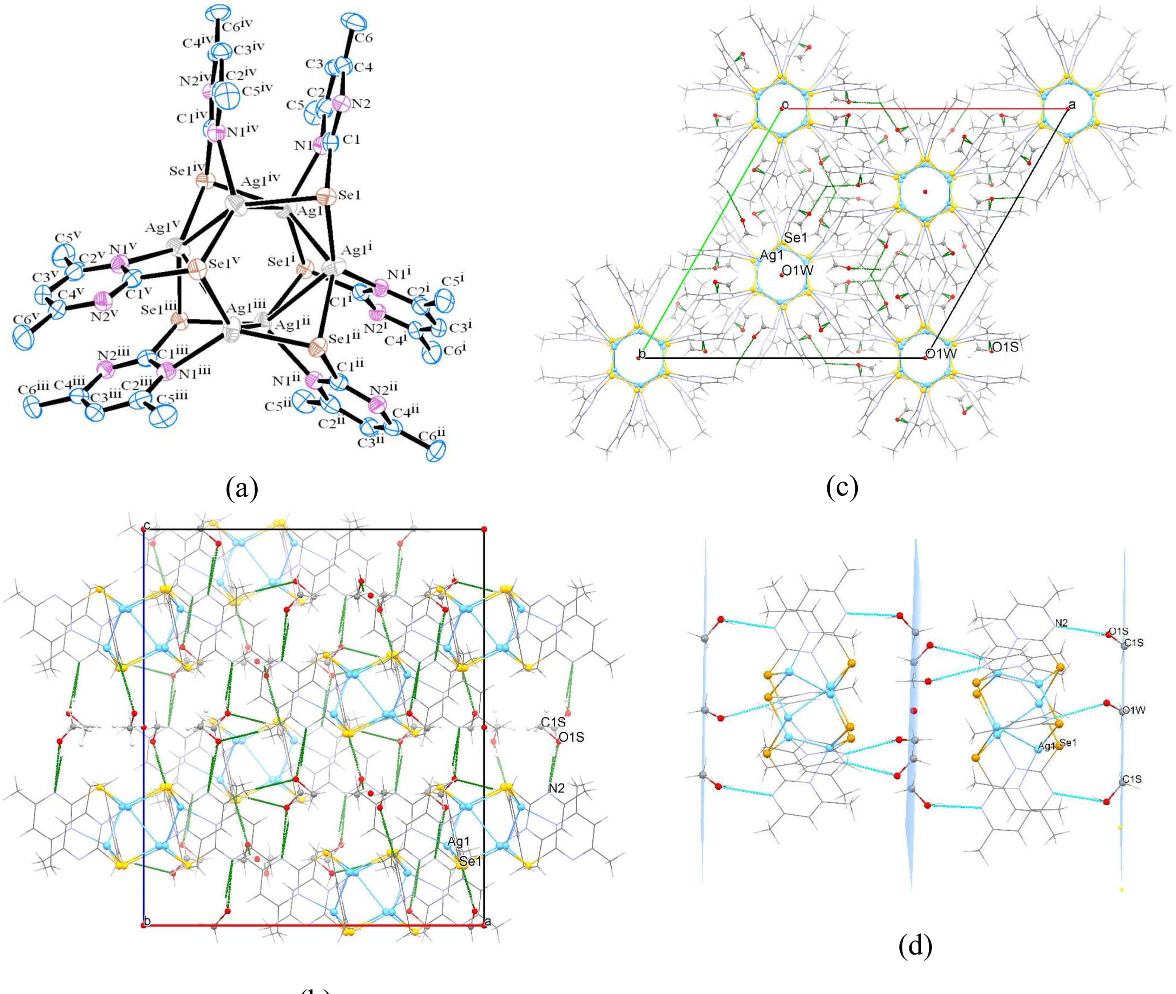

(a)

(c)

(b)

(d)

Fig. 2 (a) Crystal structure of $[Ag\{SeC_4H(Me\text{-}4,6)_2N_2\}]_6.6MeOH.H_2O$ (**2.**6MeOH.H$_2$O) with atomic number scheme (ellipsoids with 25 % probability) (hydrogen atoms, methanol and water molecules are exclude for clarity) (b) packing along *b*-axis plane (c) packing along *c*-axis (d) arrangement of water molecule with respect to methanol molecules and AgSe molecule.

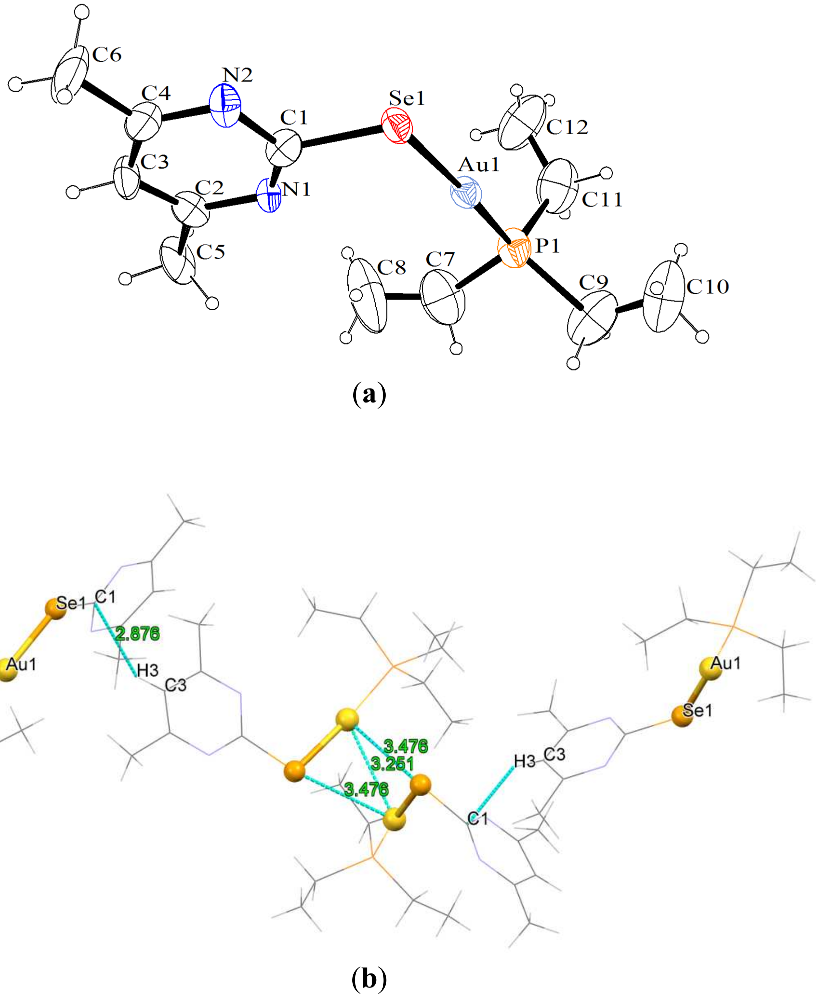

Fig. 3 (a) Crystal structure of [Au{$SeC_4H(Me\text{-}4,6)_2N_2$}($Et_3P$)] (**3**) with atomic number scheme. The ellipsoids were drawn at the 50% probability. Selected interatomic parameters: Au1– P1 = 2.276(6) Å, Au1– Se1 = 2.418(3) Å, Au1– Au1 = 3.251(2) Å, Se1– C1 = 1.88(2) Å, ∠P1 –Au1– Se1 = 175.37(18), ∠P1– Au1– Au1 = 110.58(17) ^{o}, ∠Se1– Au1– Au1 = 175.37(18) ^{o} and ∠C1– Se1– Au1 = 102.8(8) ^{o}. (b) intermolecular interaction.

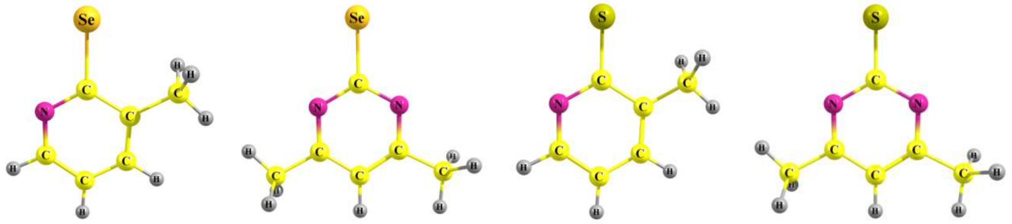

Pyridyl selenolate Pyrimidyl selenolate Pyridyl thiolate Pyrimidyl thiolate

Fig. 4 Optimized structures of bare ligands.

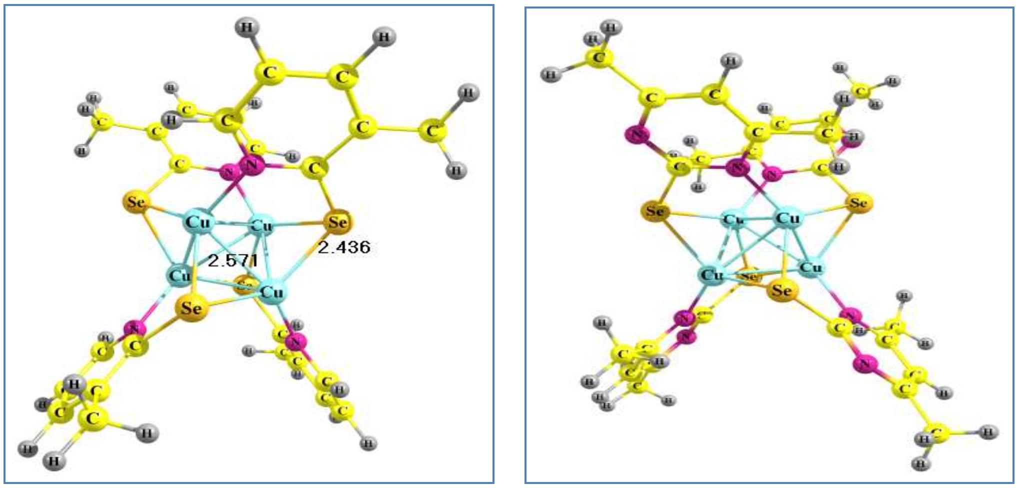

Pyridyl selenolate Pyrimidyl selenolate

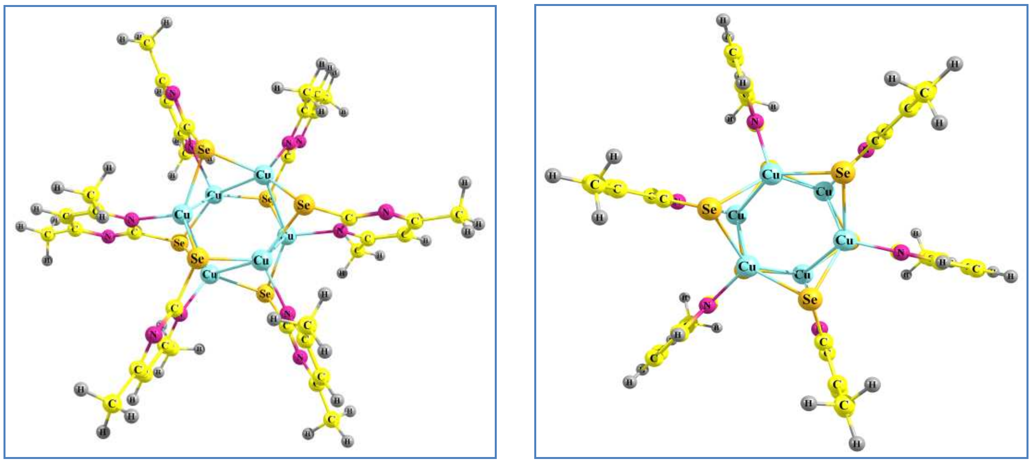

Pyrimidyl selenolate Pyridyl selenolate

Fig. 4 Optimized structures of copper pyridyl/ pyrimidyl selenolates .

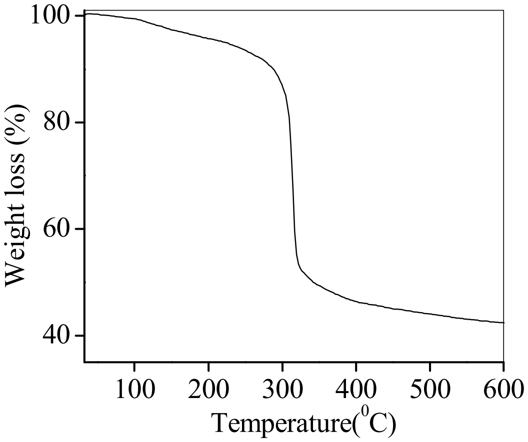

Fig. 6 TG curve of [Cu{$SeC_4H(Me\text{-}4,6)_2N_2$}]$_6$ (**1**).

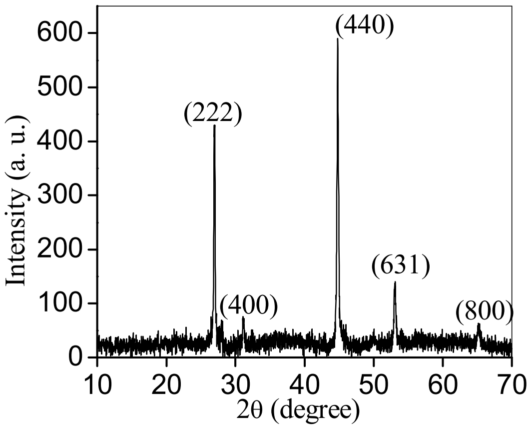

(a)

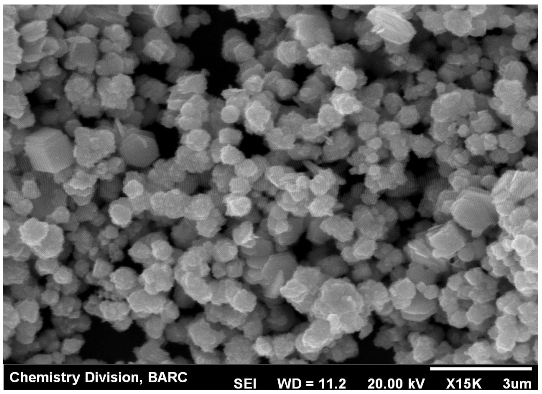

(b)

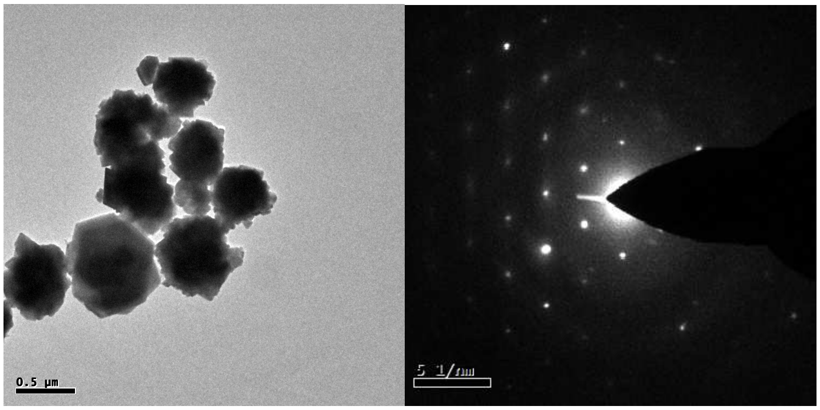

(c)

Fig. 7 a) XRD pattern, b) SEM image, c) TEM image and d) SAED pattern of Cu_7Se_4 obtained by the pyrolysis of $[Cu\{SeC_4H(Me\text{-}4,6)_2N_2\}]_6$ (**1**) in DDT at 150 °C for 25 min.

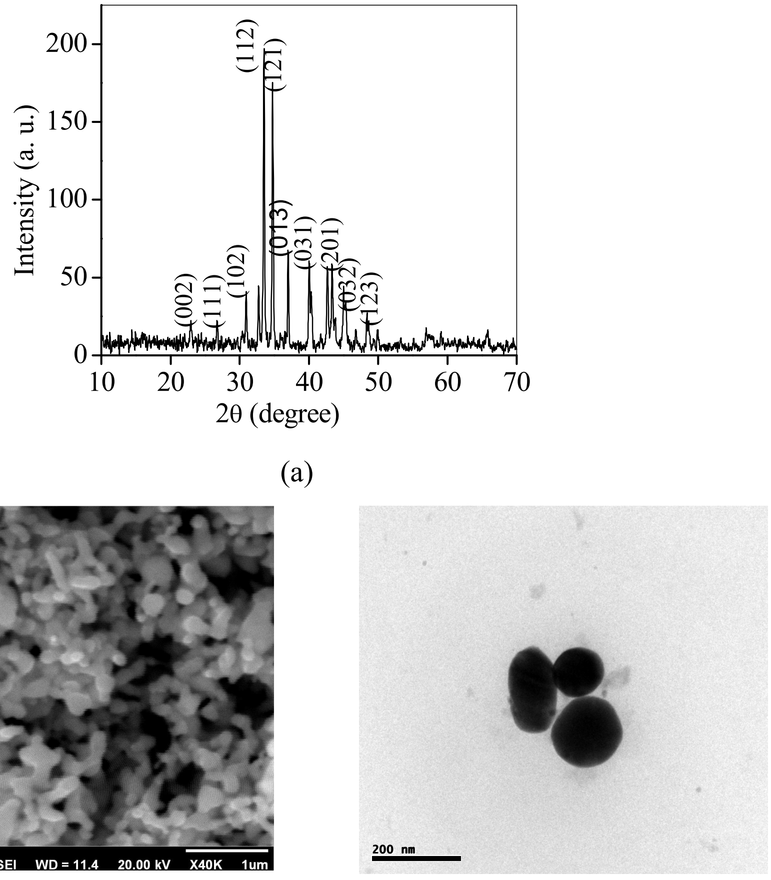

(a)

(b)

(c)

Fig. 8 a) XRD pattern, b) SEM image and c) TEM image of Ag_2Se obtained by the pyrolysis of $[Ag\{SeC_4H(Me\text{-}4,6)_2N_2\}]_6$ (**2**) in DDT/DDT at 150°C for 30 min.

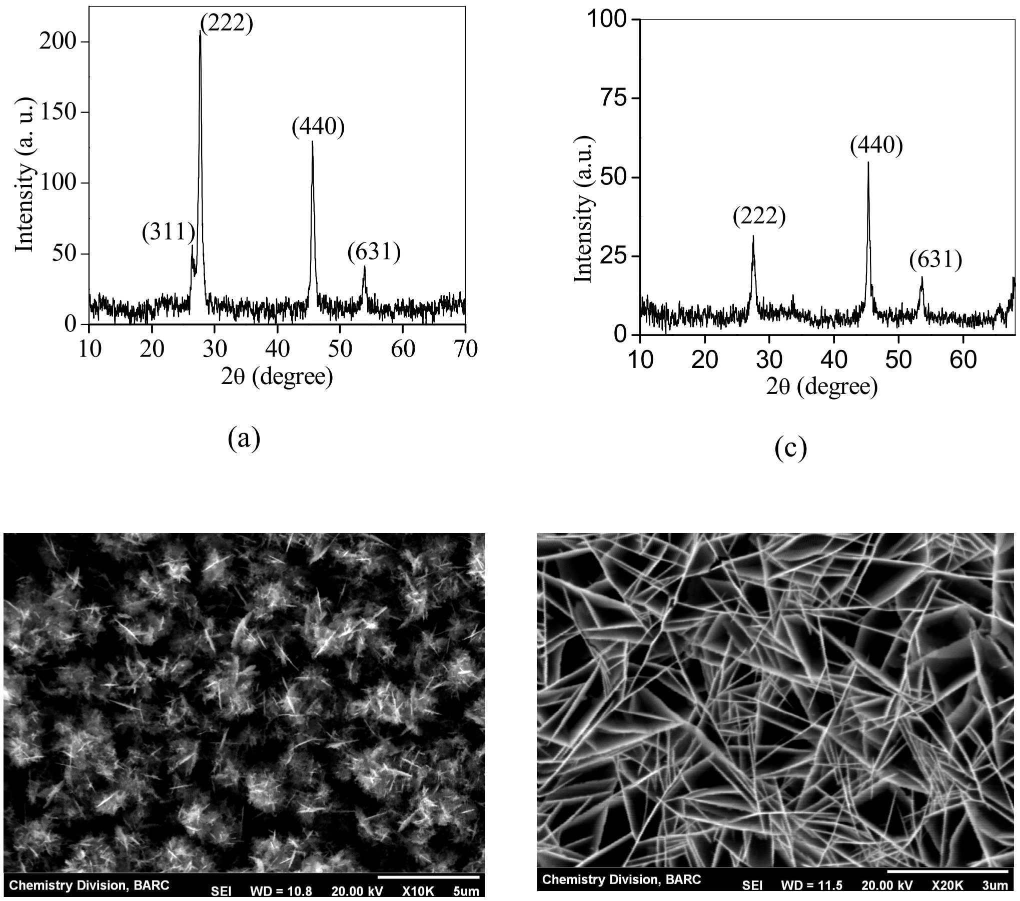

(a) (c)

(b) (d)

Fig. 9 (a) XRD pattern and b) SEM image of copper selenide (Cu_7Se_4) thin film obtained by AACVD of $[Cu\{SeC_4H(Me\text{-}4,6)_2N_2\}]_6$ (**1**) 400 °C for 3 h on glass substrate; (c) XRD and (d) SEM image of Cu_7Se_4 thin film obtained by AACVD of $[Cu\{SeC_4H(Me\text{-}4,6)_2N_2\}]_6$ (**1**) 400 °C for 3 h on silicon substrate.

Table of contents

Synthesis, structures and DFT calculations of 2-(4,6-dimethyl pyrimidyl)selenolate complexes of Cu(I), Ag(I) and Au(I) and their conversion into metal selenide nano-crystals

Rakesh K. Sharma, Amey Wadawale, G. Kedarnath, Debashree Manna, Tapan K. Ghanty, B. Vishwanadh and Vimal K. Jain*

Dimethyl pyrimidylselenolate complexes of Cu(I), Ag(I) and Au(I) were synthesized and utilized as precursors for preparation of the respective metal selenide nanostructures and thin films. DFT calculations to rationalize nuclearity in copper(I) chalcogenolate complexes suggest that the energies of tetrameric and hexameric forms are almost similar.